

MMIC BASED OPTICAL MODULATOR DESIGN

M.T. Camargo Silva* and P. R. Herczfeld

Center for Microwave-Lightwave Engineering
Drexel University, Philadelphia, Pa. 19104

ABSTRACT

The work presented in this paper concerns the development of an MMIC based optical modulator, a key element of the chip level integration of photonic and microwave components. The fundamental interaction between microwaves and light is depletion of carriers, which modulates the index of refraction. The carrier modulation gives rise to a field induced grating, which yields a modulated optical signal.

INTRODUCTION

The basic motivation of this research is the merging photonic and microwave componentry (or devices) on an MMIC substrate. The work presented here concerns the development of an optical output port. The function of an optical output port, as illustrated in Figure 1, is to bring information out of the MMICs by optical means. The concept introduced here involves sending an optical carrier via a fiber to the GaAs chip where the MMIC generated information is superimposed on the optical carrier. Finally, the coded optical signal is brought out of the chip via the fiber for processing or routing it onward as necessary. This requires the development of an MMIC based external optical modulator, which is described below.

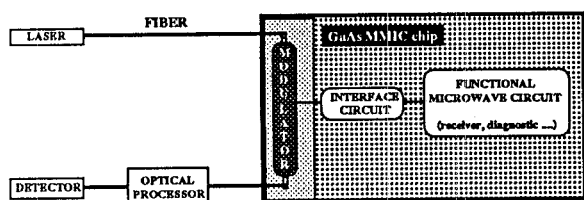


Figure 1. MMIC based external optical modulator to retrieve information from MMIC chips.

Commonly used external modulators are based on the principle of electrooptic effect to "slow down" the photons. Unfortunately, the electrooptic effect is very small; therefore, either large fields or long interaction lengths, or both, are required to introduce substantial phase modulation. Most devices use an interferometric layout, usually of the Mach-Zender type, to convert the phase (velocity) modulation into amplitude modulation. The choice of material is LiNbO_3 , which is not a semiconductor and therefore not suitable for chip level integration with electronics.

An alternate avenue for the index modulation is the use of carrier injection or depletion. The dielectric constant, and hence the index of refraction, is a function of the carrier concentration, that can be changed by injection or depletion of electrons or holes. Three effects contribute to the alteration of the refractive index: the plasma (PL), the band filling (BF), and the band-gap shrinkage (BS). Faist [1], reported analytical results for the refractive index change of GaAs, which for a n-doped material and at an optical wavelength of $1.3 \mu\text{m}$ is given by:

$$\Delta n(\text{PL}) = -3.0014 \times 10^{-21} N \quad (1)$$

$$\Delta n(\text{BF}) = -2.3908 \times 10^{-21} N \quad (2)$$

$$\Delta n(\text{BS}) = +7.4167 \times 10^{-22} N \quad (3)$$

$$n = n_0 + \Delta n \quad (4)$$

where $N(\text{cm}^{-3})$ represents the carrier concentration, n_0 is the refractive index of the undoped material. The value of n_0 was taken from Adachi [2], which reported a model for the refractive index of GaAs and GaAlAs.

Carrier injection/depletion can yield a larger change in the index of refraction than the electrooptic effect. Giguere [3], has already used the carrier induced effects on refractive index to make photonic devices.

MODULATOR STRUCTURE

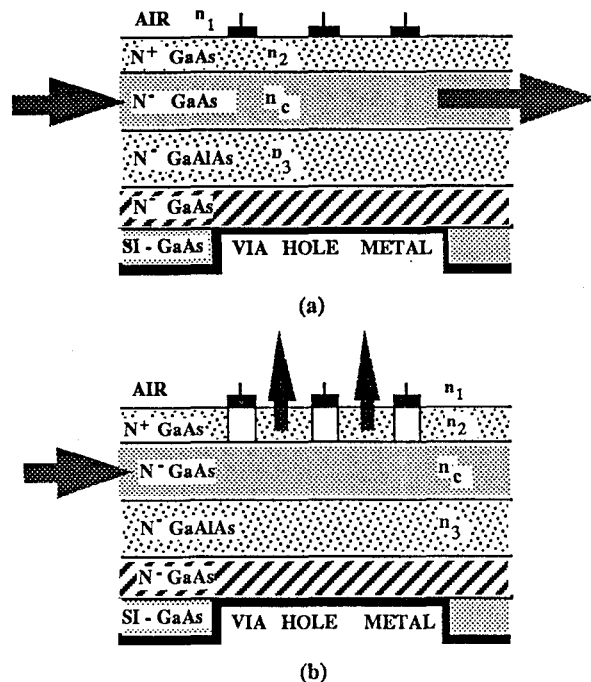
One of the several device configurations now under consideration is shown in Figure 2. The structure consists of five layers: a semi-insulating substrate (SI-GaAs), an epi-grown buffer layer, a $\text{Ga}_{0.70}\text{Al}_{0.30}\text{As}$ layer serving as a cladding, and another layer of GaAs, topped by a heavily doped active layer which also serves as a cladding. The thickness, doping density and other characteristics of each layer is summarized in Table I. The device is protected by the customary passivation layer. The periodic metallization pattern on the top of the device provides Schottky contacts. The ground electrode, at the bottom of the device, is etched into the substrate.

The device operation is as follows. Initially, in the absence of applied electric field, the light coupled into the GaAs core layer, is guided through the device, as illustrated in Figure 2a. When an electric field is applied between the electrodes, the carriers under the Schottky contacts are depleted, inducing a periodic variation of the index of refraction--a grating. The electrically modulated grating will excite leaky (radiating) modes, as illustrated in Figure 2b, instituting a modulated optical output.

TABLE I - DEVICE SPECIFICATIONS

LAYER	FUNCTION	DOPG (cm^{-3})	INDEX of REF.	THICK. (μm)
N^+GaAs	ACT. CLAD.	10^{18}	3.4453	0.06
N^-GaAs	CORE	10^{14}	3.45	0.33
$\text{N}^-\text{Ga}_{0.7}\text{Al}_{0.3}\text{As}$	CLADDING	10^{14}	3.3	2.0
N^-GaAs	BUFFER	10^{14}	3.45	1.0
SI - GaAs	SUBSTRATE	10^8	NA	100

An analytic study with computer simulation of this structure was carried out. The calculation has three main component, such as: (i) design of a suitable optical waveguide within the MMIC, (ii) design of the electric field induced periodic structure (grating), and (iii) calculation of the voltage requirement for the carrier depletion for this structure. These calculations are presented in the following sections.



2. MMIC based optical modulator. In the off state, figure 2a, the optical signal is guided uninterrupted through the device. The applied electric field depletes carriers under the Schottky contacts and thus forming a grating which scatters the light out of the guide, Figure 2b.

DESIGN OF THE OPTICAL WAVEGUIDE

To calculate the optical propagation conditions for the planar structure shown in Figure 2, we assumed that the passive cladding and the air form semi-infinite layers. For guided modes two cases need to be considered:

$$\text{i. } k_0 n_c \geq k_0 n_2 \geq \beta \geq k_0 n_3, \text{ and}$$

$$\text{ii. } k_0 n_c \geq \beta \geq k_0 n_2$$

where β is the longitudinal propagation constant. The second case is not feasible because of the large thickness of the core. For the first case the solution of the wave equation yield the customary transcendental equation:

$$T = \frac{1}{h_c} \left[\tan^{-1} \left(\frac{h_3}{h_c} \right) + \tan^{-1} \left(\frac{h_2}{h_c \tan \gamma} \right) + m\pi \right] \quad (5)$$

where m is the mode order ($m = 0, 1, 2, 3, \dots$), and h_c , h_2 , and h_3 are the transversal propagation constant of the core, the active and the passive cladding layers, respectively. These can be written:

$$h_c = k_0(n_c^2 - n_{\text{eff}}^2)^{1/2} \quad (6)$$

$$h_2 = k_0(n_2^2 - n_{\text{eff}}^2)^{1/2} \quad (7)$$

$$h_3 = k_0(n_3^2 - n_{\text{eff}}^2)^{1/2} \quad (8)$$

and

$$\gamma = \left[\tan^{-1} \left(\frac{h_2}{h_1} \right) + h_2 a \right] \quad (9)$$

where $h_1^2 = k_0^2(n_{\text{air}}^2 - n_{\text{eff}}^2)^{1/2}$ is the transversal propagation constant in the air, λ_0 is the free space wavelength and $k_0 = 2\pi/\lambda_0$.

The dispersion diagram for the first two guided modes of the waveguide simulated with the above refractive indices and $a = 0.06 \mu\text{m}$ is shown in Figure 3.

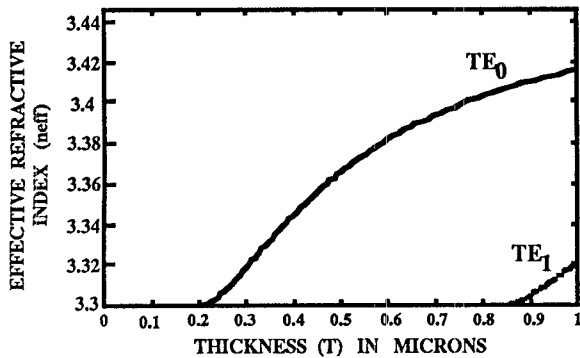


Figure 3. Dispersion diagram of the optical waveguide with the specifications given in Table I.

Figure 3 reveals that the waveguide is single-mode for $0.2 \leq T \leq 0.85 \mu\text{m}$. Simulations for confinement factor and propagation loss were also carried out. The confinement factor, i.e. the ratio of the intensity in the layer under consideration to the total intensity, for the single mode range of the waveguide is shown in Figure 4. On the basis of the results shown in this figure it may be noted that for a core thickness of $T = 0.33 \mu\text{m}$

the maximum confinement factor in the active cladding is 2%. This assures an optimum interaction between the photon field and the grating. The effective refractive index, i.e. the propagation constant with which the mode travels ($n_{\text{eff}} = \beta/k_0$), for the chosen core dimension, is 3.3267.

The propagation loss in the waveguide is due to the material absorption. The absorption data for the GaAs was obtained by linear extrapolation of measurements reported by Spitzer [4], and for GaAlAs it was calculated from the propagation loss reported by Deri [5] and Takeuchi [6] for rib type optical waveguides. The total propagation loss, shown in Figure 5, for the waveguide with $T = 0.33 \mu\text{m}$ thickness is 0.57 dB/cm. It is due primarily to the heavily doped active cladding.

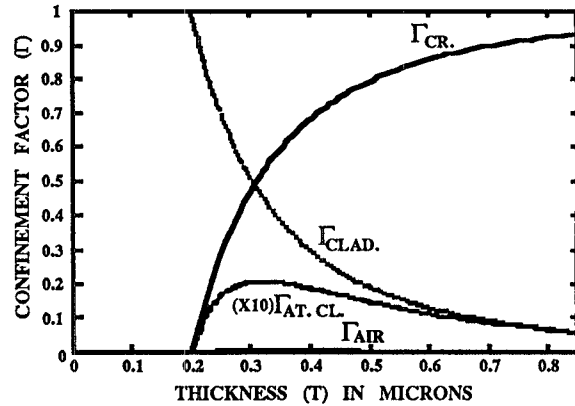


Figure 4. Confinement factor for single mode waveguide. The confinement factor of the active cladding is multiplied by ten for clarity.

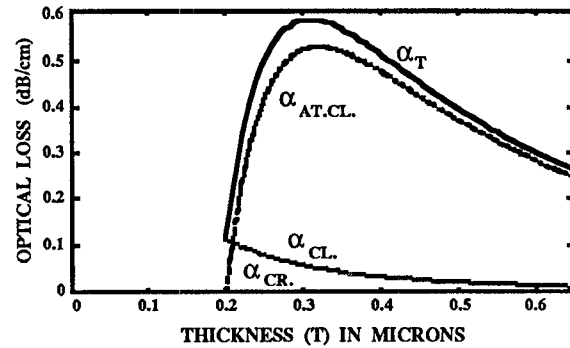


Figure 5. Waveguide propagation loss v.s. thickness.

DESIGN OF THE PERIODIC STRUCTURE

For the present design with a free space wavelength of 1.3 μm , the period for a first order grating is 200 nm; 100 nm metal finger separated by a 100nm gap. For a third order grating, the period must be of the order of 600 nm (300nm metal fingers separated by a 300 nm gaps).

VOLTAGE REQUIREMENT

The voltage required to deplete carriers at a Schottky junction is:

$$V = (qNW^2/2\epsilon_s) - V_{bi} \quad (10)$$

where, W is the depletion thickness, N is the doping density, q is the electronic charge, ϵ_s is the material permittivity, and V_{bi} is the built-in potential.

Our calculations indicate that a microwave potential of 1.6 volts is required to completely deplete the carriers in the active cladding region. Since the structure is capacitive the current requirement is negligible. Preliminary results shows that the sensitivity of the device is critically dependent on the various geometric dimensions, particularly that of the grating. The estimated modulation bandwidth, not including the parasitics is estimated to be in the GHz range. Clearly the parasitic effects will erode the performance. In general, the structure is very promising, but the various parameters have to be optimized.

CONCLUSION

The approach for a novel optical modulator presented here is rooted in GaAs MMIC technology, which, however, will require refinement and extension. To confine light into guiding regions will require a more extensive use of heterostructures, resulting in a more complex structure in the vertical direction. With the increasing sophistication of molecular beam epitaxy and related techniques, this should not present a problem. In some cases, feature sizes for the photonic devices in the lateral direction have to be in the order of a half wavelength, or just over .2 micron in GaAs. Fortunately, nanostructure fabrication is a rapidly developing technique [7], and, in the near future,

submicron feature sizes should become feasible. As feature sizes shrink, the transport of free carriers will be dominated by quantum effects, changing the basic interaction between electrons and photons. All these developments represent exciting scientific challenges to be fulfilled by the emergence of novel devices and new applications.

ACKNOWLEDGMENT

The authors wish to thank the financial support of the Brazilian Secretary of Science and Technology - RHA Program - Grant # 111/90 and NSF Grant # INT 900 - 2289.

REFERENCES

1. J. Faist and F. K. Reinhart, "Phase Modulation in GaAs/AlGaAs Double Heterostructures. I. Theory", *J. Appl. Phys.*, vol. 67, pp. 6898 - 7005, 1990.
2. S. Adachi, "GaAs, AlAs, and AlGaAs: Material Parameters for Use in Research and Device Applications", *J. Appl. Phys.*, vol. 58, pp. R1 - R29, 1985.
3. S. R. Giguere, L. Friedman, R. A. Soref, and J. P. Lorenzo, "Simulation Studies of Silicon Electro-Optic Waveguide Devices", *J. Appl. Phys.*, vol. 68, pp. 4964 - 4970, 1990.
4. W. G. Spitzer and J. M. Whelan, "Infrared Absorption and Electron Effective Mass in n-Type GaAs", *Phys. Rev.*, vol. 114, pp. 59 - 63, 1959.
5. R. J. Deri, E. Kapon, and L. M. Schiavone, "Scattering in Low-Loss GaAs/AlGaAs Rib Waveguides", *Appl. Phys. Lett.*, vol. 51, pp. 789 - 791, 1987.
6. H. Takeuchi and K. Oe, "Low-Loss Single Mode GaAs/AlGaAs Miniature Optical Waveguides with Straight and Bending Structures", *J. Lightwave Tech.*, vol. 7, pp. 1044 - 1054, 1987.
7. Proceedings of the IEEE: Special Issue on Nanoelectronics, August 1991.

*Permanent Address: Department of Electrical Engineering, Engineering School of São Carlos, University of São Paulo, São Carlos, SP 13560 Brasil.